Dissipative Solitons in Microresonators

Chapter 9
Dissipative solitons in microresonators

Cristina Rimoldi, Bennet Fischer, Luigi Di Lauro, Mario Chemnitz, Alessia Pasquazi, David J. Moss, and Roberto Morandotti

Abstract In this Chapter we will illustrate the state-of-art in the generation of dissipative solitons in Kerr microresonator-based systems. After a brief introduction on the origin of this field of research, we will discuss the modeling of these microcavities using the generalized Lugiato-Lefever equation. Further, we will discuss the different techniques used for dispersion engineering in these systems. We will then focus on the description of the frequency combs generated by microring resonators in the Kerr soliton regime and illustrate different schemes that have been developed in this context to grant better control of the microcavity dynamics. Finally, we will review the large number of applications that these objects have originated in several fields of optics.

9.1 Introduction

In the past 10 years, microresonators have revolutionized the field of optics with several applications in sensing [1–3], spectroscopy [4, 5], communication [6–9], astronomy [10, 11], and quantum optics [12–20]. These devices, generally featuring a high quality (Q) factor, can be realized under many forms, such as micro-toroids [21], spheres [22, 23], disks [24], rods [25], and integrated ring resonators [26, 27]. Further, they have been studied in many different materials, such as calcium [28] and magnesium [29] fluorides (CaF_2, MgF_2, respectively), lithium niobate ($LiNbO_3$)

C.Rimoldi · B. Fischer · L. Di Lauro · M. Chemnitz · R. Morandotti (✉)

INRS-EMT, 1650 Boulevard Lionel Boulet, Varennes, Quebec J3X 1S2, Canada

A. Pasquazi

Emergent Photonics (Epic) Laboratory, Department of Physics and Astronomy, University of Sussex, Brighton BN1 9RH, United Kingdom

D. J. Moss

Centre for Microphotonics, Swinburne University of Technology, Hawthorn, Victoria VIC 3122, Australia

e-mail: morandotti@emt.inrs.ca

[30], aluminum nitride (AIN) [31], tantalum pentoxide (Ta_2O_5) [32], silica glass [33], diamond [34], silicon [26, 35], silicon nitride (Si_3N_4) [36], oxynitrides (SiO_xN_x) [37], and high-index glass [38, 39], each offering specific advantages (and disadvantages) depending on the considered application. While these devices and materials have since been thoroughly investigated for the generation of frequency combs [40–42], the first direct demonstration of dissipative solitons in microresonators only dates back to 2014 [29], building upon the first experimental observation of Kerr solitons in a fiber cavity [43]. Kerr solitons arise from the mutual interplay of, on the one hand, dispersion and nonlinearity, and on the other hand, gain and losses. The resulting broadband frequency combs exhibit a high level of coherence, which is of fundamental importance for applications in spectroscopy, communications, and quantum measurements, as illustrated later in this Chapter.

Frequency combs, generated through cascaded four-wave mixing (FWM) in the microresonator blue-detuned regime, can exhibit either an aperiodic temporal waveform, due to arbitrary and constant phases of the comb lines, or coherent sidebands with a low repetition rate and reduced bandwidth [28, 44]. In contrast, soliton frequency comb lines display synchronized phases with higher repetition rates and bandwidths, thus resulting in an extremely narrow pulsed temporal shape [29, 45, 46]. Differently from solitons generated through mode-locked laser techniques exploiting incoherent pumping schemes, Kerr soliton frequency combs present the pump frequency within their spectrum and their generation does not make use of saturable absorbers for stabilization [47, 48]. The first experimental demonstration of dissipative Kerr solitons (DKSs) in microresonators [29] was performed in an MgF_2 crystal driven by a continuous wave (CW) pump laser. Here, solitons were observed when the optical system undergoes the transition between the effectively blue- and red-detuned regimes. In particular, while scanning for decreasing values of pump frequency, the system first displays primary sidebands in the frequency domain due to FWM, which are then followed by secondary lines. When the broadband radio-frequency (RF) signal transitions to a low-noise beatnote, a series of discrete steps in the transmission is observed and identified as a clear sign of the generation of Kerr solitons, which were then temporally characterized by the authors through frequency-resolved gating (i.e. FROG measurements). While for the general description of the microresonator system dynamics we refer the reader to [49], in the following we are going to discuss the details of the most used modeling approaches.

9.2 Modeling

The generation of dissipative Kerr solitons in microresonators can be described by means of the Lugiato-Lefever equation [50, 51] (LLE). This model was first developed for the description of pattern formation in the transverse plane (i.e., the plane

orthogonal to the propagation direction) of a Kerr medium, contained in a high-finesse cavity [50]. It is derived from Maxwell's equations considering nonlinear contributions, under paraxial, slowly varying amplitude, and mean-field approximations in the low-transmission limit [52, 53].

Years after its original formulation, the model was then adapted towards its highly successful temporal/longitudinal version [51] by Haelterman *et al.*, where the diffraction is replaced by the group velocity dispersion term and two independent temporal variables are introduced, the time t and the retarded time $t - z/v_g$, where v_g represents the group velocity and z is the propagation direction. Such a formulation describes a field that is uniform in the transverse plane while propagating along the cavity. A form equivalent to the temporal/longitudinal LLE, with quantities related to the parameters of a microring resonator (MRR), is the following

$$\frac{\partial E}{\partial t} = F - E - i\delta E + i|E|^2 E - i\frac{\beta}{2}\frac{\partial^2 E}{\partial \theta^2}$$

where E is the electric field and F is the optical injected field amplitude. The detuning term δ between the cavity frequency ω_0 and the closest input frequency ω_p is normalized to the cavity decay rate and β is proportional to the group velocity dispersion $(\partial v_g/\partial\omega)_{\omega=\omega_0}$, while the time variable t is normalized to the cavity decay time. The azimuthal angle is defined as $\theta = z/R$, where R is the MRR radius, and z is the propagation variable [54, 55]. Note that for any solution of the LLE in the above form with periodic boundary conditions in $-\pi < \theta < \pi$, θ will then need to be substituted by $\theta - (v_g/R)t$ [52].

While most early descriptions of Kerr frequency comb generation have often employed coupled mode theory (CMT) for the description of FWM in the frequency domain, the LLE, which can also be derived from CMT [54, 56], was later used to give a picture of the mean field in the temporal domain [57]. Indeed, although CMT equations offer an easy control of frequency-dependent absorption and coupling terms, they do not give direct access to the information in the time domain, which is instead easily obtained through the LLE [56]. Further, the LLE, which can be easily described as a driven, detuned, and damped nonlinear Schrödinger equation, allows for the straightforward inclusion of additional terms for Raman scattering and higher-order dispersion, as we will discuss in more detail in the following sections. On the other hand, thermo-optic effects, which can represent a limitation for Kerr combs in MRRs [58], have been successfully modeled in some systems through coupled mode equations [59, 60] as well as using the LLE [29]. For the modeling of resonator dynamics through CMT, we refer the reader to [40, 61].

9.2.1 Higher-order dispersion

In some experimental cases, solitons with sufficiently short temporal duration exhibit a spectral bandwidth that extends towards the normal dispersion region. Such solitons cannot be properly described through the LLE in the above-mentioned form, which in fact needs to be adjusted (in its temporal version [40, 51]) through the addition of higher-order dispersion terms of the form [62]

$$D_n = i^{n+1}\frac{\beta_n}{n!}\frac{\partial^n E}{\partial \tau^n}$$

for $n > 2$, where β_n is the n-th order dispersion coefficient and τ is a time variable, proportional to the previously mentioned retarded time. These additional terms allow for the modeling of soliton bandwidth restrictions in realistic cavities as well as dispersive wave generation [55], where the soliton repels a fraction of its energy into a radiant mode, an effect that can be interpreted as the optical analog of Cherenkov radiation. Additionally, higher-order dispersion mediates the interplay between FWM and dispersive wave formation, in turn giving rise to a spectral recoil, where the soliton spectral peak shifts from the original pump frequency [62, 63]. Finally, we would like to point out that higher-order dispersion terms are often accompanied by a self-steepening effect, as described in [64].

9.2.2 Raman effect

The Raman effect in microresonators has been demonstrated to be non-negligible in specific materials, such as Si_3N_4 and silica [65]. This effect is usually modeled in the LLE as a fraction of the cubic nonlinearity of the form [66]

$$f_R h_R \otimes |E|^2 \approx f_R|E|^2 - f_R\tau_R\frac{\partial|E|^2}{\partial\tau}$$

often approximated to first order [65], where f_R is the Raman fraction, h_R represents the Raman response function, and τ_R is the Raman shock time. In microresonators, the effect of Raman scattering implies the development of a self-frequency shift, where the soliton peak frequency is redshifted with respect to the CW pump laser frequency. The compensation of this shift through the spectral recoil generated by higher-order dispersion has been studied in [65]. Additionally, a new type of soliton, called Stokes soliton, has been demonstrated in the presence of Raman gain [67]. In terms of Kerr frequency comb generation, it is important to note that stimulated Raman scattering can ultimately limit the temporal and spectral width of dissipative Kerr solitons [68].

9.3 Dispersion engineered cavity dynamics

One of the key advantages of waveguide-integrated MRRs is the large variety of wavelength dispersion properties determining the linear propagation characteristics of the optical modes. In contrast to the unilateral geometries of whispery-gallery mode and photonic belt resonators [69, 70], the bilateral optical mode confinement in MRR opens a large variety of possibilities to adjust the dispersion properties of the circumventing modes. These include (a) adjusting the dimensions of the waveguide cross-section [71–73] or geometry (e.g. split or "race-track" waveguide) [14, 74], as well as (b) altering the composition of the waveguide core (see e.g. the recent works about Kerr combs in $LiNO_3$ [75], SiO_xN_y [44, 76, 77], Si_3N_4 [78], Diamond, Si) or the coating/cladding materials [36, 72]. While a very detailed overview of emerging materials for integrated microcavities is given in the comprehensive reviews by Kovach *et al.* [79] and Kippenberg *et al.* [47], here we aim to summarize the essentials of dispersion engineering in waveguide-based MRRs and its advantages for altering the temporal dynamics of DKSs.

9.3.1 Capabilities of dispersion engineering

The key for dispersion engineering in optical waveguides is a careful balance between material- and mode-specific waveguide dispersion. The choice of appropriate core, cladding, and cover layer materials alters the modal dispersion, while defining the guidance and dispersion constraints given by the individual material refractive indices. However, the waveguide geometry (i.e., cross-section and dimensions) may significantly change the modal confinement, increase the field overlap to the surrounding material (i.e. cladding [36] or cover layer [72]), and thus vary the dispersive properties of the mode. Moreover, the lithographic fabrication of photonic on-chip waveguides allows for the incorporation of gaps or slot layers, which add even more free parameters towards tailoring both dispersion and nonlinearity [80, 81]. In general, an appropriate choice of the waveguide materials, geometry, and dimension enables a plethora of dispersion landscapes, ranging from flat normal (i.e. without zero-dispersion) to anomalous dispersion with one, two, or even more zero-dispersion wavelengths in the vicinity of the pump field [81–83]. Commercially available numerical finite-element solvers are required to find the eigenmodes of the Maxwell's equations in the boundary problem imposed by the rectangular waveguide cross-sections of the MRRs. However, limitations in the fabrication processes, such as material inhomogeneity, stress built-up, and lithographic mask imperfections, usually limit the range of accessible design parameters. On the positive side, recent years have seen a considerable improvement in the fabrication processes (e.g., hybrid material systems, stress release patterns, mask improvements) [47, 79] enabling ever more access to novel dispersion regimes.

9.3.2 Advanced control of dissipative soliton dynamics

Dispersion engineering allows waveguide-integrated optical MRR to unlock unprecedented application capabilities. Transferring operation concepts such as controlled dispersive wave emission [84–86], tailored higher-order mode coupling [87–89], and soliton molecule formation [90–93] from nonlinear fibers to MRR has enabled the observation and advanced control over the dynamics of many different cavity soliton states in recent years. In the following, we are going to highlight a few of these advances.

Beyond theoretical modeling, physical limitations in the microcavity design, such as higher-order dispersion or dispersive nonlinearity, severely impact the formation of solitons in terms of bandwidth, power, and mode order. Multiple numerical and experimental studies propose practical approaches in order to optimize Kerr comb properties. In silicon nitride systems, for example, changes as small as a few hundred nm in the waveguide dimension can lead to a significant extent of the anomalous dispersion region causing a fivefold spectral extension of the Kerr comb [94]. The same study also demonstrated the selection of a suitable pump wavelength as a practical tool to alter the Kerr comb spectral extent and power after device fabrication. If pump wavelength tuning remains inaccessible, fine detuning of the free spectral range (FSR), bandwidth, and number of DKS through controlled heating of the MRR can offer an attractive alternative [95]. Similar advantages at faster tuning rates might be offered in the near future by second-order nonlinear materials such as $LiNO_3$-based MRRs [75]. Another promising approach on the fabrication side are multi-layer (slot) waveguides [81, 96] and non-uniform MRRs [97] that allow for the accurate adjustment of the cavity net-dispersion and nonlinearity, ultimately granting precise control over higher-order dispersion terms.
Such terms (i.e. $\beta_n > \beta_2$) have been demonstrated to significantly boost the comb bandwidth through one-sided or two-sided dispersive wave generation [36, 81, 98]. Dispersive wave generation is a nonlinear optical conversion process that requires a soliton-like optical pump with a flat phase in order to fulfill the phase-matching condition [62, 99]

$$\Delta\beta = \beta - \beta_s - (\omega - \omega_s)\beta_{1,s} - \frac{1}{2}\gamma_0 P_s = 0$$

The condition compares the flat phase of a soliton $\beta_s + \frac{1}{2}\gamma_0 P_s$ (with nonlinear parameter γ_0 and soliton peak power P_s) with the propagation constant of a linear wave $\beta(\omega)$ in the moving frame of the soliton $(\omega - \omega_s)\beta_{1,s}$ (with ω and ω_s angular frequencies of the linear wave and soliton respectively, and $\beta_{1,s}$ the group dispersion of the soliton), which accounts for the group velocity mismatch. The broadband spectra generated by the interplay of dispersive wave and soliton are of fundamental

use for optical metrology [36, 100] as well as future spectroscopic applications similar to [4, 101, 102]. However, due to the nature of this radiation, the dispersive part of the spectrum does not contribute to the pulsed waveform of the Kerr soliton and thus constitutes a considerable energy loss to the soliton. Moreover, it causes the soliton to spectrally shift in order to compensate for the momentum loss (known as the soliton recoil effect). Depending on the application of the comb system, these effects might be detrimental and worth being reduced through proper dispersion design.

Finally, we like to highlight an unprecedented consequence of dispersion engineering in microcavities, which is the reduction of thermal noise in so-called quiet soliton combs [103, 104]. A comprehensive study recently revealed that operating in a cavity-specific ideal dispersion domain can reduce the thermal instabilities of soliton states up to 60 dB (with 15 dB improvement experimentally shown), thus drastically stabilizing the comb repetition rate and long-term stability [104].

9.3.3 Novel phenomena in dispersion-tailored microring resonators

Advanced access to waveguide properties also enables the observation of a few unique effects of which no real equivalent exists in optical fiber systems. One of these effects is dispersive wave generation induced by avoided mode-crossing. Avoided mode-crossings may occur in waveguides with relatively large dimensions, which support more than one (fundamental) transversal mode per polarization (i.e., usually TE_{00} and TM_{00}) within the bandwidth of the optical source. Here, the avoided intersections of two transversal modes cause a significant change of the individual mode dispersions (see Fig. 1a), which can be a few orders of magnitude stronger than any other waveguide-intrinsic dispersion change and perturb soliton formation. Similar effects were observed between two different polarization modes [105].

Since larger waveguide sizes are a necessity for anomalous dispersion and power scaling of DKSs [78], intermodal crossings are very likely to occur in MRRs. However, for the purpose of favorable power scaling of cavity solitons, energy leakage due to non-solitonic radiation is largely undesired. Efforts to decrease the impact of higher-order modes include the incorporation of tapered sections into the MRRs [78, 97] as well as higher-order mode isolation couplers [106].

On the contrary, it is noteworthy that mode-crossings, in turn, host the unique capability to steer dispersive-wave formation, since they provide a strong variation of the dispersion. Thus, such crossings eventually provide a set of well defined, very narrow wavelength regions of perfect phase-matching between a soliton pump (in the transversal mode 1) and a dispersive wave (in the transversal mode 2) [103,

107]. Hence, the involvement of avoided mode-crossings imposes advantages on (i) the tuneability of the overall comb bandwidth, (ii) the accurate spectral relocation of dispersive wave energy, as well as (iii) refining the temporal characteristics of the dispersive radiation. Most notably, tailored narrow-band mode-crossings were utilized for the highly efficient generation of dispersive radiation into a single resonator mode (see Fig. 1b) [103]. The study reports further on hysteresis-like interaction between this strong mode and the spectro-temporal behavior of the soliton as well as on the ability of repetition rate stabilization (so-called quiet states), which clearly hosts advantages for switching and long-term stable applications.

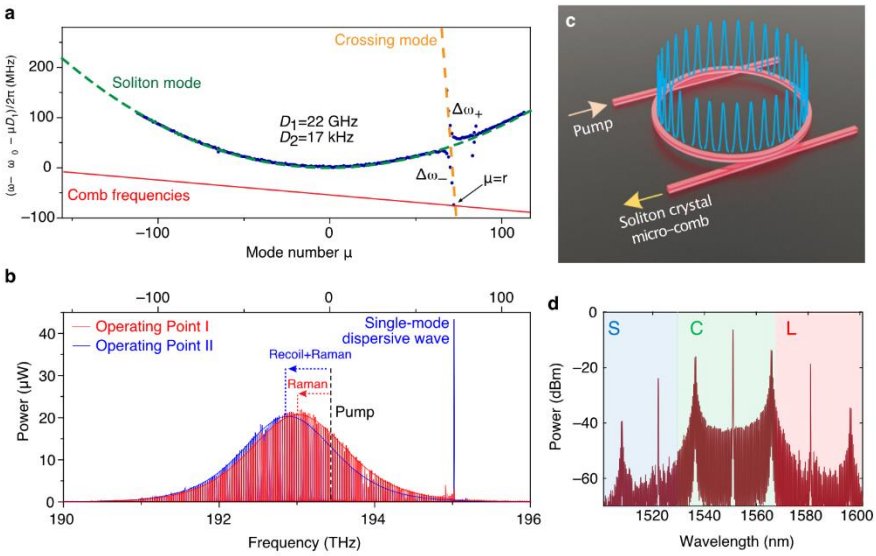

Fig. 1 a). Dispersion of a cavity soliton with avoided mode-crossing. **b)** Spectrum of soliton comb featuring a single-mode dispersive wave (blue). (a-b) adapted (labels, font size and line widths) from [103] under CC BY 4.0 license. **c)** Illustration of a soliton crystal state and **d)** respective measured spectrum. (c-d) adapted (font size) from [108] under CC BY 4.0 license.

A further specialty of MRRs is the greater ability to reach stable control over the formation of multi-soliton states. Here, mastering of cavity stability through a balance of dispersion, nonlinearity, gain and loss, allows for the formation of multiple cavity solitons. In particular, the fine control over the dispersive properties of the cavity via thermal tuning as fast as 100 μs ultimately enables an on-demand increase of the soliton number and the controlled study of multi-soliton behavior [95]. These achievements resulted in the observation and active control of soliton crystals [33, 109]. Here, nonlinear nearest neighbor interactions allow phase-locked multi-photon states distributed over an equidistant temporal grid. The robustness of this highly ordered temporal alignment, in combination with the control over spacing and the existence of vacancies (i.e. Schottky defects) in the temporal grid, gives rise to the name *soliton crystals* in analogy to solid-state atomic crystals. The narrow spacing

of the solitons in the MRR allows for a very practical indirect read-out through their spectra. For instance, through straight-forward Fourier transform rules, the number of solitons in the crystal can be read from the FSR of the most dominant cavity modes, while the number and positions of vacancies become apparent from the underlying modulation structure of the secondary modes (see Fig. 1c,d). The manifold of crystal states and their robustness open up unique and unprecedented applications, among which we can mention background-free soliton lasers with GHz repetition rates [110], ultra-dense data transmission for telecommunications [111], as well as activation functionalities for photonic neural networks [108].

9.4 Soliton comb generation schemes

Although Kerr frequency combs promise a powerful alternative to fiber-based frequency comb systems, they come with certain limitations that prevent their widespread use. Indeed, the generation of Kerr combs and their reliable long-term stabilization is currently one of the major bottlenecks that prevent a successful commercialization. In particular, DKSs (a subgroup of Kerr combs) are of high interest for a variety of applications due to their inherent GHz [112] to THz [113] repetition rates, short pulse durations, as well as their high phase stability between comb lines. In order to reach stable soliton operation, several different techniques have been developed in recent years and are briefly described below. For a more thorough review of soliton comb generation schemes, see for example refs. [16, 40, 47, 114].

In general, the majority of developed schemes rely on a tunable narrow linewidth CW laser source that is swept into the microcavity to reach the red-detuned soliton operation point. In 2013, Matsko *et al.* theoretically showed how to achieve DKSs through continuous scanning of the pump frequency, from blue-detuned to red-detuned values (i.e. from a higher optical frequency to a lower optical frequency with zero detuning from the center of the resonance) [115], as was also reported in later works [29, 64, 116]. When an MRR reaches a regime that allows for the propagation of stable DKSs, the intra-cavity energy experiences a sudden drop in intensity. The understanding of this behavior led to the demonstration of DKSs in microresonators in 2014 by Herr *et al.* [29]. These were previously observed in 2013 by Saha *et al.* under the form of femtosecond stable pulses in Si_3N_4 MRRs [117].

In 2009, Strekalov and Yu proposed a pumping scheme based on the use of a bichromatic source to produce frequency combs in MgF_2 MRRs, exploiting cascaded FWM rather than optical parametric generation [118, 119], leading to highly efficient DKS generation. Similarly, an electro-optic pumping scheme was exploited by Papp *et al.* [120, 121], which has experimentally shown the realization and control of extremely precise equidistant comb lines, essential for achieving ultra-stable solitons.

Additionally, techniques adapted from classical metrology such as the locking of the carrier-envelope-offset (CEO) frequency via self-referencing (i.e. *f*-2*f* interferometry [122]) of the generated comb have been investigated in order to obtain fully stabilized frequency combs in a compact footprint [123, 124]. Towards long-term stabilization, several techniques such as Pound-Drever-Hall feedback control systems [103], servo feedback loops [125], or sideband modulation [126, 127] have been explored.

9.4.1 Frequency scanning

Initial schemes have utilized a simple, yet effective technique in order to overcome the issue of thermal cavity drifts [29, 115]: By shifting the CW laser source from the blue- to the red-detuned regime, an intracavity thermal equilibrium can be reached, allowing the stable generation of soliton combs. Here, the sweeping speed of the laser is crucial for the generation of the soliton combs and should match the microcavities photon and thermal lifetime, which can be difficult to achieve for some material platforms. As described earlier, the detuning of the pump starting from the blue side leads first to a primary frequency comb, formed through the intracavity power build-up, which in turn seeds FWM within the cavity. Further detuning of the pump laser results in to the generation of 'subcombs' and unstable combs formed by modulation instabilities (MI). The common feature of these combs in the blue-detuned regime is high noise in the RF-domain, due to multiple and broad RF beatnotes arising from MI. Once the red-detuned regime is reached, the intracavity power shows an abrupt decline in power and the so-called *soliton steps* can be observed, which show characteristic step sizes depending on the chosen material platform. Here, the generated solitons feature very narrow RF beatnotes as well as stable optical comb outputs. At the beginning of this regime, multi-soliton states are generated and, with increased detuning, they subsequently break down until a single soliton-state is reached. The goal of the frequency scanning method is, to stop the frequency detuning of the laser, once the single soliton state is obtained, which is easier achievable if the soliton step-sizes feature longer time durations (~ms for e.g. MgF_2 [29]).

9.4.2 Power Kicking

The power-kicking method [36, 128] is a widely used technique that allows for the generation of soliton combs in materials that feature a high thermo-optic coefficient. In these materials (such as Si_3N_4), the observed soliton steps exhibit very short time durations (~µs), which prevent the effective use of the frequency scanning method (i.e. to precisely stop the laser frequency on one of the soliton steps). Instead of

using only a single tunable CW laser, two intensity modulators (acousto-optic and electro-optic modulators, AOM and EOM, respectively) are included before the microcavity. The use of the EOM is necessary to obtain the required speed, which cannot be provided by the AOM alone. Here, the AOM reduces the pump power of the source before tuning into the resonance, allowing to quickly reach the soliton steps. Subsequently, the AOM increases the pump power in order to stabilize the reached soliton step. After the AOM, an EOM helps diminishing thermal instabilities by effectively reducing the pump power right before the zero-detuning point (i.e. the resonance center), which also ensures a fast transition to the soliton steps. When the settings (and timings) for the laser frequency sweeping and both modulations are correctly chosen, this method allows for the reliable generation of soliton combs in materials featuring higher thermo-optic coefficients.

9.4.3 Thermal Tuning

A more inexpensive method can be realized with on-chip resistive heaters on top of the microcavities [95, 129]. In this scheme, the tunable CW laser is replaced by a fixed frequency CW laser diode and the cavity resonance is thermally tuned by inducing a refractive index change caused by the thermo-optic effect. This can be realized through, for example, an electrode on top of the microcavity, which is current controlled. This allows for relatively fast speeds (given the small structure and thermal mass of the electrode) as well as for the fine tuning precision (determined by the bit-depth of the used digital-to-analog converter) required to directly obtain the short (~µs) soliton steps. Furthermore, although similar to the frequency scanning scheme, the thermal tuning technique offers advantages due to the use of single frequency lasers with lower RF noise as well as narrower linewidths (compared to tunable lasers), resulting in combs with lower noise. However, for use in more complex photonic integrated circuits (PICs), local heating of the chip might pose additional restrictions as other integrated elements would need to be shielded from any temperature gradients and effects (i.e. thermal crosstalk), thus potentially limiting the scope of this technique [130].

9.4.4 Self-injection locking and laser-based configurations

The previously reported schemes rely on the use of CW lasers for pumping, which are far from being monochromatic sources (with linewidth shifts of tens of kHz), suffer from instabilities due to noise, and require extensive optical pump power (~ Watt level), as well as elaborate feedback control systems. Additionally, thermal instabilities can strongly affect the ability to generate and stabilize coherent states,

since solutions may experience thermal drifting, hence, leading to the destruction of the coherent soliton regimes.

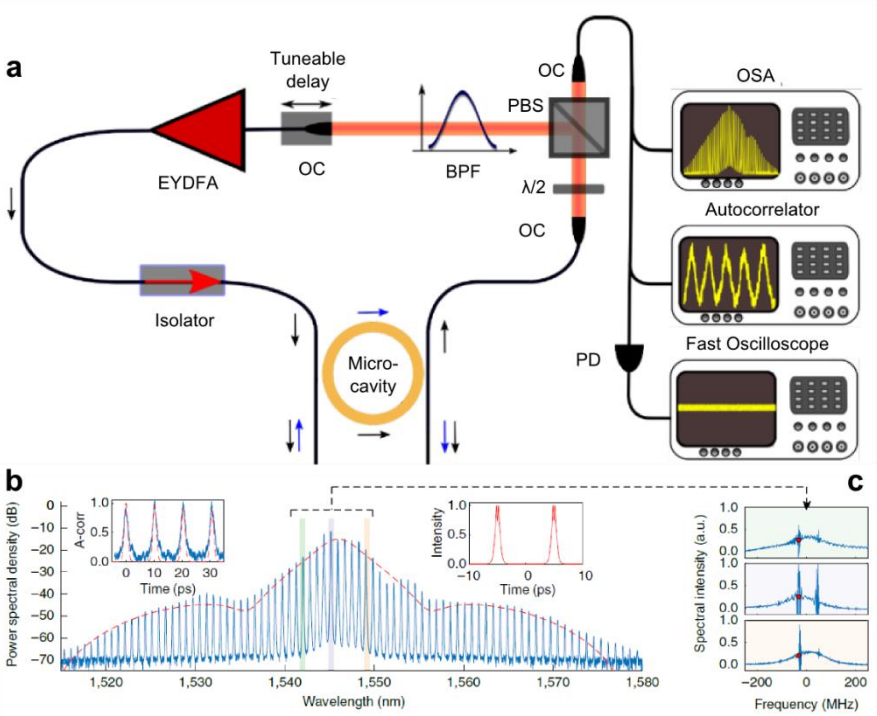

Fig. 2 Nested cavity setup for soliton generation. a) The setup consists of a high-doped index silica glass (Hydex) MRR (Microcavity) nested in an external feedback fiber cavity, composed of a short-length erbium-ytterbium co-doped fiber amplifier (EYDFA), an optical isolator to ensure unidirectional propagation, a tunable optical bandpass filter (BPF), a tunable delay line, a polarizer (PBS), a waveplate (λ/2) for polarization control and three optical collimators (OCs). The external propagation cavity modes sustain the microcavity pulses, which are broadened by the Kerr non-linearity over the gain bandwidth. This setup allows to reach stable soliton states with a variable repetition rate in the order of megahertz. **b)** Soliton generation for two equidistant solitons per round-trip, with 150 mW output power from the amplifier and 30 mW output from the MRR. The experimental (blue) and theoretical (red) values of the spectrum measured with an optical spectrum analyzer (OSA) and autocorrelation trace are shown in the left and right insets, respectively. The temporal intensity output from the fiber cavity is monitored with a photodiode (PD) and a fast oscilloscope **c)** Intracavity spectrum (blue), showing the mode lasing within each microcavity resonance. Adapted (cropped with modified font size and labels) with permission from figures (3,S6) in Bao *et al.* Nature Photonics 13: 384-389 [110].

Thermo-optical nonlinearity, originating from the thermal capacitance of the micro-resonator material, modifies the steady-state solutions of the intra-cavity field, by creating a slow dependence of the refractive index from the temperature. This, in turn, induces an additional detuning with respect to the pump frequency, which competes with the ultra-fast Kerr red-shift, resulting in a variety of non-solitonic

nonlinear regimes, such as self-pulsing and deterministic chaos [49, 60, 85, 115, 131–134].

In order to address stabilization issues, Yi *et al.* [125] proposed an active approach by employing a feedback loop for the self-adjustment of the output power. Such a configuration allowed to achieve coherent states that are robust against thermal instabilities over long times. This in turn led to the development of even more efficient schemes that allow for the generation of stable solitons through passive driving and control of the cavity parameters, known as passive self-injection locking. This technique was proposed in an initial work by Liang *et al.,* to narrow the linewidth of a distributed feedback laser with an MRR [135].

Injection-locking schemes based on free-running diode lasers have gained increased interest for the use in simplified, small footprint turn-key soliton generators [136–139]. Here, instead of using a tunable CW laser for pumping (which needs to be optically isolated from the microcavity – a difficult task for monolithic integration), the microcavity is directly attached to a semiconductor laser diode (e.g. a distributed feedback laser, DFB), which is operated in a free-running mode. Small back-reflections inside the microcavity are being utilized to lock the free-running diode to the microcavity resonance, which subsequently allows for stable soliton generation.

In 2020, Shen *et al.* demonstrated a turn-key soliton comb generator based on a DFB laser coupled to a Si_3N_4 microresonator chip packaged inside a commercially available butterfly package [138]. The authors showed reliable soliton comb generation with an FSR of 40 GHz spanning 30 nm, requiring only 30 mW of optical pump power. Remarkably, the demonstrated system not only allows for reliable turn-key operation (meaning that repeated on and off switching results in the same comb output) but it also exhibits much lower noise figures than other monolithic integrated lasers and even off-the-shelf tunable external cavity lasers.

In 2019, Bao and coauthors used a nested cavity configuration scheme for producing Kerr solitons [110, 133, 140], based on a nested configuration where an MRR is embedded in an external fiber cavity, which allows for signal reinjection into the ring.

This setup, illustrated in Fig. 2, is inspired by a passive laser mode-locking setup, first demonstrated by Pasquazi, Peccianti *et al.* in 2012 [40, 141–146], which embeds an MRR in an active laser loop. The result is a mode-locking almost insensitive to thermally-induced fluctuations. Remarkably, Bao *et al.* recently demonstrated a new class of DKSs that can be generated upon a free-CW background, with a tunable repetition rate of megahertz, sustained by the gain of the lasing medium, with a mode efficiency of 75% at average powers that are one order of magnitude lower than the energy threshold for soliton generation predicted by the LLE [110].

9.5 Nonlinear dynamics of DKS

Cavity solitons in MRRs can exhibit a rich variety of nonlinear dynamical regimes and intriguing nonlinear effects that have been exploited in a plethora of practical applications in spectroscopy, sensing, and telecommunications (see the following section for more details). Some examples of the available regimes are bright and dark solitons states [147], soliton Cherenkov radiation [62], Stokes solitons [67], as well as soliton crystallization [109, 111, 148], switching [149], and breather states [150, 151].

Bright and dark solitons can coexist in Kerr media that undergo third-order dispersion in the normal regime, as studied by Parra-Rivas *et al.* [152]. Indeed, Xue and coauthors have shown that dark soliton states can be observed in the normal dispersion regime [153]. Moreover, as outlined earlier, Brasch *et al.*, reported that higher-order dispersion terms in silicon nitride MRRs, while inducing a spectral broadening of the coherent states, can enable Cherenkov radiation associated to DKS propagation [36]. Stokes solitons have been also observed in MRRs, where their generation is mediated by the compensation process between Raman interaction and dispersion, which supports stable soliton propagation [47]. This is achieved through the exchange of energy with a primary DKS, formed via Kerr nonlinearity, and Stokes states, belonging to a distinct mode family.

Remarkably, in 2019, Karpov *et al.* demonstrated the generation of deterministic soliton crystal states in MRRs for a critical pump power value, corresponding to a stable defect-free lattice of optical pulses, sustained by the modulated driving field of a CW source [154]. The investigation of soliton crystals revealed the interesting dynamical features stemming from the switching of these states into transient chaos and the formation of breathers via a melting and recrystallization process.

9.6 Applications

Since their first introduction in 2007 [155], Kerr frequency combs (incl. soliton combs) have gained increased interest as a powerful, small-scale alternative to traditional frequency combs [122, 156], arising from their potentially low power consumption [113] as well as their cost-efficient, mass producible integration through the same CMOS-processes and infrastructure of the semiconductor industry [80]. Moreover, as outlined earlier, the generated Kerr frequency combs can eventually span, depending on the chosen material platform and dispersion engineering, the ultraviolet [157, 158], the visible [159], the mid-infrared [160], up to the THz regimes [161], offering great opportunities for many fields of application. Further, the capability of precisely adjusting the dispersion allows for the generation of combs that can intrinsically cover more than one octave (where a frequency and its double

both exist within the generated spectrum, e.g. 150 THz (~2 μm) and 300 THz (~1 μm)), avoiding the need for further broadening in a preceding nonlinear device, which is important for comb stabilization [98, 124] and crucial for most of their intended applications. As a result of this versatility, Kerr soliton frequency combs have already revolutionized many applications, including classical frequency comb adaptions such as dual-comb spectroscopy [4]. Moreover, due to the small structures of microcavities, high FSRs (ranging from GHz to THz) can be achieved, which makes these platforms interesting for telecommunications applications. In fact, the FSRs of microcavities can be finely adjusted to match the WDM (wavelength division multiplexing, 100 GHz) and DWDM (dense WDM, 50 GHz) telecom grids, thus allowing for massively parallel and high-bandwidth transmission schemes obtained by exclusively using a single optical source [9, 111]. Other novel concepts and demonstrations include optical clockworks/gears, which are able to coherently link different electromagnetic domains, e.g. from hundreds of THz to MHz. This in turn allows the optical frequency of an atomic reference (e.g. Rb) to be counted by standard electrics [162–164]. Besides, promising applications including optical frequency synthesizers [165], RF processing [166], ultra-fast and multicolor optical ranging (i.e. LIDAR, light detection and ranging) [167–169], the generation of THz radiation [161], as well as astrocombs [10, 11, 170] have been all demonstrated, to only name a few.

More recently, advanced 'hybrid' approaches such as the combination of microcavities with piezo-electric materials [169], opto-mechanical designs [171], and integrated MRRs in electro-optic materials [75] have been investigated, offering new possibilities and functionalities for these powerful microcavity platforms.
Finally, it is noteworthy that besides the aforementioned soliton applications, microcavities have attracted significant attention for utilization outside the soliton regime in applications such as biosensing [172, 173], narrow-linewidth lasers schemes [174], optical machine-learning [108, 175–178], and quantum technologies [13, 15, 17, 18, 179–184].

References

1. Vollmer F, Braun D, Libchaber A, et al (2002) Protein detection by optical shift of a resonant microcavity. Appl Phys Lett 80:4057–4059. https://doi.org/10.1063/1.1482797
2. Arnold S, Khoshsima M, Teraoka I, et al (2003) Shift of whispering-gallery modes in microspheres by protein adsorption. Opt Lett 28:272. https://doi.org/10.1364/OL.28.000272
3. Armani AM (2010) Single molecule detection using optical microcavities. In: Chremmos I, Schwelb O, Uzunoglu N (eds) Photonic Microresonator Research and Applications. Springer US, Boston, MA, pp 253–273
4. Suh M-G, Yang Q-F, Yang KY, et al (2016) Microresonator soliton dual-comb spectroscopy. Science 354:600–603. https://doi.org/10.1126/science.aah6516

5. Yu M, Okawachi Y, Griffith AG, et al (2017) Microresonator-based high-resolution gas spectroscopy. Opt Lett 42:4442. https://doi.org/10.1364/OL.42.004442
6. Pfeifle J, Brasch V, Lauermann M, et al (2014) Coherent terabit communications with microresonator Kerr frequency combs. Nat Photonics 8:375–380. https://doi.org/10.1038/nphoton.2014.57
7. Liang W, Eliyahu D, Ilchenko VS, et al (2015) High spectral purity Kerr frequency comb radio frequency photonic oscillator. Nat Commun 6:7957. https://doi.org/10.1038/ncomms8957
8. Nguyen TG, Shoeiby M, Chu ST, et al (2015) Integrated frequency comb source based Hilbert transformer for wideband microwave photonic phase analysis. Opt Express 23:22087. https://doi.org/10.1364/OE.23.022087
9. Marin-Palomo P, Kemal JN, Karpov M, et al (2017) Microresonator-based solitons for massively parallel coherent optical communications. Nature 546:274–279. https://doi.org/10.1038/nature22387
10. Obrzud E, Rainer M, Harutyunyan A, et al (2019) A microphotonic astrocomb. Nat Photonics 13:31–35. https://doi.org/10.1038/s41566-018-0309-y
11. Suh M-G, Yi X, Lai Y-H, et al (2019) Searching for exoplanets using a microresonator astrocomb. Nat Photonics 13:25–30. https://doi.org/10.1038/s41566-018-0312-3
12. Lefèvre-Seguin V, Haroche S (1997) Towards cavity-QED experiments with silica microspheres. Mater Sci Eng B 48:53–58. https://doi.org/10.1016/S0921-5107(97)00080-9
13. Reimer C, Kues M, Roztocki P, et al (2016) Generation of multiphoton entangled quantum states by means of integrated frequency combs. Science 351:1176–1180. https://doi.org/10.1126/science.aad8532
14. Okawachi Y, Yu M, Luke K, et al (2016) Quantum random number generator using a microresonator-based Kerr oscillator. Opt Lett 41:4194. https://doi.org/10.1364/OL.41.004194
15. Kues M, Reimer C, Lukens JM, et al (2019) Quantum optical microcombs. Nat Photonics 13:170–179. https://doi.org/10.1038/s41566-019-0363-0
16. Wang F, Wang W, Niu R, et al (2020) Quantum key distribution with on-chip dissipative Kerr soliton. Laser Photon Rev 14:1900190. https://doi.org/10.1002/lpor.201900190
17. Reimer C, Zhang Y, Roztocki P, et al (2018) On-chip frequency combs and telecommunications signal processing meet quantum optics. Front Optoelectron 11:134–147. https://doi.org/10.1007/s12200-018-0814-0
18. Caspani L, Reimer C, Kues M, et al (2016) Multifrequency sources of quantum correlated photon pairs on-chip: a path toward integrated quantum frequency combs. Nanophotonics 5:351–362
19. Reimer C, Kues M, Caspani L, et al (2015) Cross-polarized photon-pair generation and bi-chromatically pumped optical parametric oscillation on a chip. Nat Commun 6:8236. https://doi.org/10.1038/ncomms9236
20. Sciara S, Roztocki P, Rimoldi C, et al (2019) Generation and processing of complex photon states with quantum frequency combs. IEEE Photonics Technol Lett 31:1862–1865. https://doi.org/10.1109/LPT.2019.2944564
21. Armani DK, Kippenberg TJ, Spillane SM, Vahala KJ (2003) Ultra-high-Q toroid microcavity on a chip. Nature 421:925–928. https://doi.org/10.1038/nature01371
22. Braginsky VB, Gorodetsky ML, Ilchenko VS (1989) Quality-factor and nonlinear properties

of optical whispering-gallery modes. Phys Lett A 137:393–397. https://doi.org/10.1016/0375-9601(89)90912-2

23. Gorodetsky ML, Savchenkov AA, Ilchenko VS (1996) Ultimate Q of optical microsphere resonators. Opt Lett 21:453. https://doi.org/10.1364/OL.21.000453
24. Yi X, Yang Q-F, Yang KY, et al (2015) Soliton frequency comb at microwave rates in a high-Q silica microresonator. Optica 2:1078. https://doi.org/10.1364/OPTICA.2.001078
25. Zhang S, Silver JM, Del Bino L, et al (2019) Sub-milliwatt-level microresonator solitons with extended access range using an auxiliary laser. Optica 6:206. https://doi.org/10.1364/OPTICA.6.000206
26. Almeida VR, Barrios CA, Panepucci RR, Lipson M (2004) All-optical control of light on a silicon chip. Nature 431:1081–1084. https://doi.org/10.1038/nature02921
27. Duchesne D, Ferrera M, Razzari L, et al (2009) Efficient self-phase modulation in low loss, high index doped silica glass integrated waveguides. Opt Express 17:1865. https://doi.org/10.1364/OE.17.001865
28. Savchenkov AA, Matsko AB, Strekalov D, et al (2004) Low threshold optical oscillations in a whispering gallery mode CaF2 resonator. Phys Rev Lett 93:243905. https://doi.org/10.1103/PhysRevLett.93.243905
29. Herr T, Brasch V, Jost JD, et al (2014) Temporal solitons in optical microresonators. Nat Photonics 8:145–152. https://doi.org/10.1038/nphoton.2013.343
30. He Y, Yang Q-F, Ling J, et al (2019) Self-starting bi-chromatic LiNbO3 soliton microcomb. Optica 6:1138. https://doi.org/10.1364/OPTICA.6.001138
31. Gong Z, Bruch A, Shen M, et al (2018) High-fidelity cavity soliton generation in crystalline AlN micro-ring resonators. Opt Lett 43:4366. https://doi.org/10.1364/OL.43.004366
32. Wu C-L, Hung Y-J, Fan R, et al (2019) Tantalum pentoxide (Ta2O5) based athermal micro-ring resonator. OSA Contin 2:1198. https://doi.org/10.1364/OSAC.2.001198
33. Lu Z, Wang W, Zhang W, et al (2019) Deterministic generation and switching of dissipative Kerr soliton in a thermally controlled micro-resonator. AIP Adv 9:025314. https://doi.org/10.1063/1.5080128
34. Hausmann BJM, Bulu I, Venkataraman V, et al (2014) Diamond nonlinear photonics. Nat Photonics 8:369–374. https://doi.org/10.1038/nphoton.2014.72
35. Griffith AG, Lau RKW, Cardenas J, et al (2015) Silicon-chip mid-infrared frequency comb generation. Nat Commun 6:6299. https://doi.org/10.1038/ncomms7299
36. Brasch V, Geiselmann M, Herr T, et al (2016) Photonic chip-based optical frequency comb using soliton Cherenkov radiation. Science 351:357–360. https://doi.org/10.1126/science.aad4811
37. Chen D, Kovach A, Shen X, et al (2017) On-chip ultra-high-Q silicon oxynitride optical resonators. ACS Photonics 4:2376–2381. https://doi.org/10.1021/acsphotonics.7b00752
38. Moss DJ, Morandotti R, Gaeta AL, Lipson M (2013) New CMOS-compatible platforms based on silicon nitride and Hydex for nonlinear optics. Nat. Photonics 7:597–607
39. Ferrera M, Duchesne D, Razzari L, et al (2012) Advanced integrated photonics in doped silica glass. Springer Ser. Opt. Sci. 47–92
40. Pasquazi A, Peccianti M, Razzari L, et al (2018) Micro-combs: A novel generation of optical sources. Phys Rep 729:1–81. https://doi.org/10.1016/j.physrep.2017.08.004
41. Caspani L, Duchesne D, Dolgaleva K, et al (2011) Optical frequency conversion in integrated

devices [Invited]. J Opt Soc Am B 28:A67. https://doi.org/10.1364/josab.28.000a67

42. Pasquazi A, Ahmad R, Rochette M, et al (2010) All-optical wavelength conversion in an integrated ring resonator. Opt Express 18:3858. https://doi.org/10.1364/oe.18.003858
43. Leo F, Coen S, Kockaert P, et al (2010) Temporal cavity solitons in one-dimensional Kerr media as bits in an all-optical buffer. Nat Photonics 4:471–476. https://doi.org/10.1038/nphoton.2010.120
44. Razzari L, Duchesne D, Ferrera M, et al (2010) CMOS-compatible integrated optical hyper-parametric oscillator. Nat Photonics 4:41–45. https://doi.org/10.1038/nphoton.2009.236
45. Herr T, Hartinger K, Riemensberger J, et al (2012) Universal formation dynamics and noise of Kerr-frequency combs in microresonators. Nat Photonics 6:480–487. https://doi.org/10.1038/nphoton.2012.127
46. Bao H, Cooper A, Chu ST, et al (2018) Type-II micro-comb generation in a filter-driven four wave mixing laser [Invited]. Photonics Res 6:B67. https://doi.org/10.1364/prj.6.000b67
47. Kippenberg TJ, Gaeta AL, Lipson M, Gorodetsky ML (2018) Dissipative Kerr solitons in optical microresonators. Science 361:eaan8083. https://doi.org/10.1126/science.aan8083
48. Caspani L, Reimer C, Pasquazi A, et al (2013) A novel integrated laser source without a laser. SPIE Newsroom. https://doi.org/10.1117/2.1201312.005240
49. Herr T, Gorodetsky ML, Kippenberg TJ (2015) Dissipative Kerr solitons in optical microresonators. In: Nonlinear Optical Cavity Dynamics. Wiley-VCH Verlag GmbH & Co. KGaA, Weinheim, Germany, pp 129–162
50. Lugiato LA, Lefever R (1987) Spatial dissipative structures in passive optical systems. Phys Rev Lett 58:2209–2211. https://doi.org/10.1103/PhysRevLett.58.2209
51. Haelterman M, Trillo S, Wabnitz S (1992) Dissipative modulation instability in a nonlinear dispersive ring cavity. Opt Commun 91:401–407. https://doi.org/10.1016/0030-4018(92)90367-Z
52. Lugiato LA, Prati F, Gorodetsky ML, Kippenberg TJ (2018) From the Lugiato–Lefever equation to microresonator-based soliton Kerr frequency combs. Philos Trans R Soc A Math Phys Eng Sci 376:20180113. https://doi.org/10.1098/rsta.2018.0113
53. Lugiato L, Prati F, Brambilla M (2015) Nonlinear optical systems. Cambridge University Press, Cambridge
54. Chembo YK, Menyuk CR (2013) Spatiotemporal Lugiato-Lefever formalism for Kerr-comb generation in whispering-gallery-mode resonators. Phys Rev A 87:053852. https://doi.org/10.1103/PhysRevA.87.053852
55. Coen S, Randle HG, Sylvestre T, Erkintalo M (2013) Modeling of octave-spanning Kerr frequency combs using a generalized mean-field Lugiato–Lefever model. Opt Lett 38:37. https://doi.org/10.1364/OL.38.000037
56. Hansson T, Modotto D, Wabnitz S (2014) On the numerical simulation of Kerr frequency combs using coupled mode equations. Opt Commun 312:134–136. https://doi.org/10.1016/j.optcom.2013.09.017
57. Matsko AB, Savchenkov AA, Strekalov D, et al (2005) Optical hyperparametric oscillations in a whispering-gallery-mode resonator: Threshold and phase diffusion. Phys Rev A 71:033804. https://doi.org/10.1103/PhysRevA.71.033804
58. Drake TE, Stone JR, Briles TC, Papp SB (2019) Thermal decoherence and laser cooling of Kerr microresonator solitons. ArXiv 1903.00431

59. Ilchenko VS, Gorodetsky ML (1992) Thermal nonlinear effects in optical whispering gallery microresonators. Laser Phys 2:1004
60. Di Lauro L, Li J, Moss DJ, et al (2017) Parametric control of thermal self-pulsation in micro-cavities. Opt Lett 42:3407. https://doi.org/10.1364/OL.42.003407
61. Chembo YK, Strekalov D V., Yu N (2010) Spectrum and dynamics of optical frequency combs generated with monolithic whispering gallery mode resonators. Phys Rev Lett 104:103902. https://doi.org/10.1103/PhysRevLett.104.103902
62. Cherenkov A V., Lobanov VE, Gorodetsky ML (2017) Dissipative Kerr solitons and Cherenkov radiation in optical microresonators with third-order dispersion. Phys Rev A 95:033810. https://doi.org/10.1103/PhysRevA.95.033810
63. Erkintalo M, Xu YQ, Murdoch SG, et al (2012) Cascaded phase matching and nonlinear symmetry breaking in fiber frequency combs. Phys Rev Lett 109:223904. https://doi.org/10.1103/PhysRevLett.109.223904
64. Lamont MRE, Okawachi Y, Gaeta AL (2013) Route to stabilized ultrabroadband microresonator-based frequency combs. Opt Lett 38:3478. https://doi.org/10.1364/OL.38.003478
65. Karpov M, Guo H, Kordts A, et al (2016) Raman self-frequency shift of dissipative Kerr solitons in an optical microresonator. Phys Rev Lett 116:103902. https://doi.org/10.1103/PhysRevLett.116.103902
66. Blow KJ, Wood D (1989) Theoretical description of transient stimulated Raman scattering in optical fibers. IEEE J Quantum Electron 25:2665–2673. https://doi.org/10.1109/3.40655
67. Yang Q-F, Yi X, Yang KY, Vahala K (2017) Stokes solitons in optical microcavities. Nat Phys 13:53–57. https://doi.org/10.1038/nphys3875
68. Wang Y, Anderson M, Coen S, et al (2018) Stimulated Raman scattering imposes fundamental limits to the duration and bandwidth of temporal cavity solitons. Phys Rev Lett 120:053902. https://doi.org/10.1103/PhysRevLett.120.053902
69. Grudinin IS, Yu N (2015) Dispersion engineering of crystalline resonators via microstructuring. Optica 2:221. https://doi.org/10.1364/optica.2.000221
70. Yang KY, Beha K, Cole DC, et al (2016) Broadband dispersion-engineered microresonator on a chip. Nat Photonics 10:316–320. https://doi.org/10.1038/nphoton.2016.36
71. Foster MA, Turner AC, Sharping JE, et al (2006) Broad-band optical parametric gain on a silicon photonic chip. Nature 441:960–963. https://doi.org/10.1038/nature04932
72. Riemensberger J, Hartinger K, Herr T, et al (2012) Dispersion engineering of thick high-Q silicon nitride ring-resonators via atomic layer deposition. Opt Express 20:27661. https://doi.org/10.1364/OE.20.027661
73. Zhang L, Bao C, Singh V, et al (2013) Generation of two-cycle pulses and octave-spanning frequency combs in a dispersion-flattened micro-resonator. Opt Lett 38:5122. https://doi.org/10.1364/ol.38.005122
74. Kim S, Han K, Wang C, et al (2017) Dispersion engineering and frequency comb generation in thin silicon nitride concentric microresonators. Nat Commun 8:. https://doi.org/10.1038/s41467-017-00491-x
75. Wang C, Zhang M, Yu M, et al (2019) Monolithic lithium niobate photonic circuits for Kerr frequency comb generation and modulation. Nat Commun 10:978. https://doi.org/10.1038/s41467-019-08969-6

76. Ferrera M, Duchesne D, Razzari L, et al (2009) Low power four wave mixing in an integrated, micro-ring resonator with Q = 12 million. Opt Express 17:14098. https://doi.org/10.1364/oe.17.014098
77. Ferrera M, Razzari L, Duchesne D, et al (2008) Low-power continuous-wave nonlinear optics in doped silica glass integrated waveguide structures. Nat Photonics 2:737–740. https://doi.org/10.1038/nphoton.2008.228
78. Kordts A, Pfeiffer MHP, Guo H, et al (2016) Higher order mode suppression in high-Q anomalous dispersion SiN microresonators for temporal dissipative Kerr soliton formation. 2016 Conf Lasers Electro-Optics, CLEO 2016 41:452–455. https://doi.org/10.1364/ol.41.000452
79. Kovach A, Chen D, He J, et al (2020) Emerging material systems for integrated optical Kerr frequency combs. Adv Opt Photonics 12:135. https://doi.org/10.1364/aop.376924
80. Leuthold J, Koos C, Freude W (2010) Nonlinear silicon photonics. Nat Photonics 4:535–544. https://doi.org/10.1038/nphoton.2010.185
81. Bao C, Taheri H, Zhang L, et al (2017) High-order dispersion in Kerr comb oscillators. J Opt Soc Am B 34:715. https://doi.org/10.1364/josab.34.000715
82. Turner AC, Manolatou C, Schmidt BS, et al (2006) Tailored anomalous group-velocity dispersion in silicon waveguides. Conf Lasers Electro-Optics 2006 Quantum Electron Laser Sci Conf CLEO/QELS 2006 14:4357–4362. https://doi.org/10.1109/CLEO.2006.4628293
83. Klenner A, Mayer AS, Johnson AR, et al (2016) Gigahertz frequency comb offset stabilization based on supercontinuum generation in silicon nitride waveguides. Opt Express 24:11043. https://doi.org/10.1364/oe.24.011043
84. Tartara L, Cristiani I, Degiorgio V (2003) Blue light and infrared continuum generation by soliton fission in a microstructured fiber. Appl Phys B Lasers Opt 77:307–311. https://doi.org/10.1007/s00340-003-1172-0
85. Chemnitz M, Scheibinger R, Gaida C, et al (2018) Thermodynamic control of soliton dynamics in liquid-core fibers. Optica 5:695. https://doi.org/10.1364/OPTICA.5.000695
86. Cristiani I, Tediosi R, Tartara L, Degiorgio V (2004) Dispersive wave generation by solitons in microstructured optical fibers. Opt Express 12:124–135. https://doi.org/10.1364/OPEX.12.000124
87. Demas J, Steinvurzel P, Tai B, et al (2015) Intermodal nonlinear mixing with Bessel beams in optical fiber. Optica 2:14. https://doi.org/10.1364/optica.2.000014
88. Wright LG, Christodoulides DN, Wise FW (2017) Spatiotemporal mode-locking in multimode fiber lasers. Science 358:94–97. https://doi.org/10.1126/science.aao0831
89. Wright LG, Christodoulides DN, Wise FW (2015) Controllable spatiotemporal nonlinear effects in multimode fibres. Nat Photonics 9:306–310. https://doi.org/10.1038/nphoton.2015.61
90. Haboucha A, Leblond H, Salhi M, et al (2008) Coherent soliton pattern formation in a fiber laser. Opt Lett 33:524. https://doi.org/10.1364/ol.33.000524
91. Amrani F, Salhi M, Grelu P, et al (2011) Universal soliton pattern formations in passively mode-locked fiber lasers. Opt Lett 36:1545. https://doi.org/10.1364/OL.36.001545
92. Grelu P, Akhmediev N (2012) Dissipative solitons for mode-locked lasers. Nat Photonics 6:84–92. https://doi.org/10.1038/nphoton.2011.345
93. Qin H, Xiao X, Wang P, Yang C (2018) Observation of soliton molecules in a spatiotemporal

mode-locked multimode fiber laser. Opt Lett 43:1982. https://doi.org/10.1364/OL.43.001982

94. Okawachi Y, Lamont MRE, Luke K, et al (2014) Bandwidth shaping of microresonator-based frequency combs via dispersion engineering. Opt Lett 39:3535. https://doi.org/10.1364/OL.39.003535
95. Joshi C, Jang JK, Luke K, et al (2016) Thermally controlled comb generation and soliton modelocking in microresonators. Opt Lett 41:2565. https://doi.org/10.1364/OL.41.002565
96. Guo Y, Jafari Z, Agarwal AM, et al (2016) Bilayer dispersion-flattened waveguides with four zero-dispersion wavelengths. Opt Lett 41:4939. https://doi.org/10.1364/ol.41.004939
97. Huang SW, Liu H, Yang J, et al (2016) Smooth and flat phase-locked Kerr frequency comb generation by higher order mode suppression. Sci Rep 6:1–7. https://doi.org/10.1038/srep26255
98. Pfeiffer MHP, Herkommer C, Liu J, et al (2017) Octave-spanning dissipative Kerr soliton frequency combs in Si3N4 microresonators. Optica 4:684. https://doi.org/10.1364/OPTICA.4.000684
99. Husakou A V, Herrmann J (2001) Supercontinuum generation of higher-order solitons by fission in photonic crystal fibers. Phys Rev Lett 87:203901. https://doi.org/10.1103/PhysRevLett.87.203901
100. Newman ZL, Maurice V, Drake T, et al (2019) Architecture for the photonic integration of an optical atomic clock. Optica 6:680. https://doi.org/10.1364/optica.6.000680
101. Yu M, Okawachi Y, Joshi C, et al (2018) Gas-phase microresonator-based comb spectroscopy without an external pump laser. ACS Photonics 5:2780–2785. https://doi.org/10.1021/acsphotonics.8b00579
102. Yu M, Okawachi Y, Griffith AG, et al (2018) Silicon-chip-based mid-infrared dual-comb spectroscopy. Nat Commun 9:6–11. https://doi.org/10.1038/s41467-018-04350-1
103. Yi X, Yang Q-F, Zhang X, et al (2017) Single-mode dispersive waves and soliton microcomb dynamics. Nat Commun 8:14869. https://doi.org/10.1038/ncomms14869
104. Stone JR, Papp SB (2020) Harnessing dispersion in soliton microcombs to mitigate thermal noise. ArXiv 2006.10907v1
105. Ramelow S, Farsi A, Clemmen S, et al (2014) Strong polarization mode coupling in microresonators. Opt Lett 39:5134. https://doi.org/10.1364/ol.39.005134
106. Yu Z, Yuhang W, Xinxuan M, et al (2019) High-order mode suppressed microresonators based on multimode waveguides and a low-loss mode remover. Front Opt - Proc Front Opt + Laser Sci APS/DLS 1:3–4. https://doi.org/10.1364/FIO.2019.JTu4A.89
107. Yang Q-F, Yi X, Yang KY, Vahala K (2016) Spatial-mode-interaction-induced dispersive waves and their active tuning in microresonators. Optica 3:1132. https://doi.org/10.1364/optica.3.001132
108. Xu X, Tan M, Corcoran B, et al (2020) Photonic perceptron based on a Kerr microcomb for high-speed, scalable, optical neural networks. Laser Photon Rev 2000070. https://doi.org/10.1002/lpor.202000070
109. Cole DC, Lamb ES, Del'Haye P, et al (2017) Soliton crystals in Kerr resonators. Nat Photonics 11:671–676. https://doi.org/10.1038/s41566-017-0009-z
110. Bao H, Cooper A, Rowley M, et al (2019) Laser cavity-soliton microcombs. Nat Photonics 13:384–389. https://doi.org/10.1038/s41566-019-0379-5
111. Corcoran B, Tan M, Xu X, et al (2020) Ultra-dense optical data transmission over standard

fibre with a single chip source. Nat Commun 11:2568. https://doi.org/10.1038/s41467-020-16265-x

112. Suh M-G, Vahala K (2018) Gigahertz-repetition-rate soliton microcombs. Optica 5:65. https://doi.org/10.1364/OPTICA.5.000065
113. Stern B, Ji X, Okawachi Y, et al (2018) Battery-operated integrated frequency comb generator. Nature 562:401–405. https://doi.org/10.1038/s41586-018-0598-9
114. Gaeta AL, Lipson M, Kippenberg TJ (2019) Photonic-chip-based frequency combs. Nat Photonics 13:158–169. https://doi.org/10.1038/s41566-019-0358-x
115. Matsko AB, Liang W, Savchenkov AA, Maleki L (2013) Chaotic dynamics of frequency combs generated with continuously pumped nonlinear microresonators. Opt Lett 38:525. https://doi.org/10.1364/ol.38.000525
116. Webb KE, Erkintalo M, Coen S, Murdoch SG (2016) Experimental observation of coherent cavity soliton frequency combs in silica microspheres. Opt Lett 41:4613. https://doi.org/10.1364/ol.41.004613
117. Saha K, Okawachi Y, Shim B, et al (2013) Modelocking and femtosecond pulse generation in chip-based frequency combs. Opt Express 21:1335. https://doi.org/10.1364/oe.21.001335
118. Strekalov D V, Yu N (2009) Generation of optical combs in a whispering gallery mode resonator from a bichromatic pump. Phys Rev A 79:. https://doi.org/10.1103/physreva.79.041805
119. Hansson T, Wabnitz S (2014) Bichromatically pumped microresonator frequency combs. Phys Rev A 90:013811. https://doi.org/10.1103/PhysRevA.90.013811
120. Papp SB, Del'Haye P, Diddams SA (2013) Parametric seeding of a microresonator optical frequency comb. Opt Express 21:17615. https://doi.org/10.1364/oe.21.017615
121. Papp SB, Beha K, Del'Haye P, et al (2014) Microresonator frequency comb optical clock. Optica 1:10. https://doi.org/10.1364/optica.1.000010
122. Udem T, Reichert J, Holzwarth R, Hänsch TW (1999) Absolute optical frequency measurement of the cesium D1 line with a mode-locked laser. Phys Rev Lett 82:3568–3571. https://doi.org/10.1103/PhysRevLett.82.3568
123. Jost JD, Herr T, Lecaplain C, et al (2015) Counting the cycles of light using a self-referenced optical microresonator. Optica 2:706. https://doi.org/10.1364/OPTICA.2.000706
124. Brasch V, Lucas E, Jost JD, et al (2017) Self-referenced photonic chip soliton Kerr frequency comb. Light Sci Appl 6:e16202–e16202. https://doi.org/10.1038/lsa.2016.202
125. Yi X, Yang Q-F, Youl Yang K, Vahala KJ (2016) Active capture and stabilization of temporal solitons in microresonators. Opt Lett 41:2037. https://doi.org/10.1364/OL.41.002037
126. Del'Haye P, Coillet A, Fortier T, et al (2015) Phase coherent link of an atomic clock to a self-referenced microresonator frequency comb. arXiv 1511.08103
127. Lamb ES, Carlson DR, Hickstein DD, et al (2018) Optical-frequency measurements with a Kerr microcomb and photonic-chip supercontinuum. Phys Rev Appl 9:024030. https://doi.org/10.1103/PhysRevApplied.9.024030
128. Brasch V, Geiselmann M, Pfeiffer MHP, Kippenberg TJ (2016) Bringing short-lived dissipative Kerr soliton states in microresonators into a steady state. Opt Express 24:29312. https://doi.org/10.1364/OE.24.029312
129. Wang W, Lu Z, Zhang W, et al (2018) Robust soliton crystals in a thermally controlled microresonator. Opt Lett 43:2002. https://doi.org/10.1364/OL.43.002002

130. Milanizadeh M, Aguiar D, Melloni A, Morichetti F (2019) Canceling thermal cross-talk effects in photonic integrated circuits. J Light Technol 37:1325–1332. https://doi.org/10.1109/JLT.2019.2892512
131. Jin L, Pasquazi A, Lauro L Di, et al (2016) Demonstration of bi- and multi-stability in a high order ring resonator. In: 2016 21st OptoElectronics and Communications Conference (OECC) held jointly with 2016 International Conference on Photonics in Switching (PS). pp 1–3
132. Jin L, Di Lauro L, Pasquazi A, et al (2020) Optical multi-stability in a nonlinear high-order microring resonator filter. APL Photonics 5:56106. https://doi.org/10.1063/5.0002941
133. Rowley M, Wetzel B, Di Lauro L, et al (2019) Thermo-optical pulsing in a microresonator filtered fiber-laser: a route towards all-optical control and synchronization. Opt Express 27:19242–19254
134. Hansson T, Modotto D, Wabnitz S (2013) Dynamics of the modulational instability in microresonator frequency combs. Phys Rev A 88:. https://doi.org/10.1103/physreva.88.023819
135. Liang W, Ilchenko VS, Savchenkov AA, et al (2010) Whispering-gallery-mode-resonator-based ultranarrow linewidth external-cavity semiconductor laser. Opt Lett 35:2822. https://doi.org/10.1364/ol.35.002822
136. Kondratiev NM, Lobanov VE, Cherenkov A V., et al (2017) Self-injection locking of a laser diode to a high-Q WGM microresonator. Opt Express 25:28167. https://doi.org/10.1364/oe.25.028167
137. Pavlov NG, Koptyaev S, Lihachev G V., et al (2018) Narrow-linewidth lasing and soliton Kerr microcombs with ordinary laser diodes. Nat Photonics 12:694–698. https://doi.org/10.1038/s41566-018-0277-2
138. Shen B, Chang L, Liu J, et al (2020) Integrated turnkey soliton microcombs. Nature 582:365–369. https://doi.org/10.1038/s41586-020-2358-x
139. Liang W, Ilchenko VS, Eliyahu D, et al (2015) Ultralow noise miniature external cavity semiconductor laser. Nat Commun 6:7371. https://doi.org/10.1038/ncomms8371
140. Bao H, Olivieri L, Rowley M, et al (2020) Turing patterns in a fiber laser with a nested microresonator: Robust and controllable microcomb generation. Phys Rev Res 2:. https://doi.org/10.1103/physrevresearch.2.023395
141. Pasquazi A, Caspani L, Peccianti M, et al (2013) Self-locked optical parametric oscillation in a CMOS compatible microring resonator: a route to robust optical frequency comb generation on a chip. Opt Express 21:13333. https://doi.org/10.1364/oe.21.013333
142. Pasquazi A, Peccianti M, Little BE, et al (2012) Stable, dual mode, high repetition rate mode-locked laser based on a microring resonator. Opt Express 20:27355. https://doi.org/10.1364/oe.20.027355
143. Bao H, Cooper A, Di Lauro L, et al (2017) Repetition rate controllable filter-driven four wave mixing laser. 2017 Conf. Lasers Electro-Optics Eur. Eur. Quantum Electron. Conf.
144. Pasquazi A, Peccianti M, Chu ST, et al (2016) Novel ultrafast sources on chip: filter driven four wave mixing lasers, from high repetition rate to burst mode operation. Laser Reson. Microresonators, Beam Control XVIII
145. Peccianti M, Pasquazi A, Park Y, et al (2012) Demonstration of a stable ultrafast laser based on a nonlinear microcavity. Nat Commun 3:765. https://doi.org/10.1038/ncomms1762
146. Pasquazi A, Peccianti M, Clerici M, et al (2014) Collapse arrest in instantaneous Kerr media

via parametric interactions. Phys Rev Lett 113:. https://doi.org/10.1103/physrevlett.113.133901

147. Weiner AM, Heritage JP, Hawkins RJ, et al (1988) Experimental observation of the fundamental dark soliton in optical fibers. Phys Rev Lett 61:2445–2448. https://doi.org/10.1103/PhysRevLett.61.2445
148. Xu X, Tan M, Wu J, et al (2020) Broadband photonic RF channelizer with 92 channels based on a soliton crystal microcomb. J Light Technol 38:5116–5121. https://doi.org/10.1109/JLT.2020.2997699
149. Guo H, Karpov M, Lucas E, et al (2016) Universal dynamics and deterministic switching of dissipative Kerr solitons in optical microresonators. Nat Phys 13:94–102. https://doi.org/10.1038/nphys3893
150. Lucas E, Karpov M, Guo H, et al (2017) Breathing dissipative solitons in optical microresonators. Nat Commun 8:736. https://doi.org/10.1038/s41467-017-00719-w
151. Matsko AB, Savchenkov AA, Maleki L (2012) On excitation of breather solitons in an optical microresonator. Opt Lett 37:4856. https://doi.org/10.1364/ol.37.004856
152. Parra-Rivas P, Gomila D, Gelens L (2017) Coexistence of stable dark- and bright-soliton Kerr combs in normal-dispersion resonators. Phys Rev A 95:. https://doi.org/10.1103/physreva.95.053863
153. Xue X, Xuan Y, Liu Y, et al (2015) Mode-locked dark pulse Kerr combs in normal-dispersion microresonators. Nat Photonics 9:594–600. https://doi.org/10.1038/nphoton.2015.137
154. Karpov M, Guo H, Pfeiffer MHP, et al (2017) Dynamics of soliton crystals in optical Microresonators. 2017 Conf. Lasers Electro-Optics, CLEO 2017 - Proc. 2017-Janua:1–2
155. Del'Haye P, Schliesser A, Arcizet O, et al (2007) Optical frequency comb generation from a monolithic microresonator. Nature 450:1214–1217. https://doi.org/10.1038/nature06401
156. Glauber RJ, Hall JL, Hänsch TW (2005) Advanced information on the Nobel Prize in Physics 2005. Quantum-mechanical theory of optical coherence - Laser-based precision spectroscopy and optical frequency comb techniques. General introduction. 1–14
157. Liu X, Bruch AW, Gong Z, et al (2018) Ultra-high-Q UV microring resonators based on a single-crystalline AlN platform. Optica 5:1279. https://doi.org/10.1364/OPTICA.5.001279
158. Dorche AE, Timucin D, Thyagarajan K, et al (2020) Advanced dispersion engineering of a III-Nitride micro-resonator for a blue/UV frequency comb. arXiv 2006.07391
159. Lee SH, Oh DY, Yang Q-F, et al (2017) Towards visible soliton microcomb generation. Nat Commun 8:1295. https://doi.org/10.1038/s41467-017-01473-9
160. Hansson T, Modotto D, Wabnitz S (2014) Mid-infrared soliton and Raman frequency comb generation in silicon microrings. Opt Lett 39:6747. https://doi.org/10.1364/OL.39.006747
161. Zhang S, Silver JM, Shang X, et al (2019) Terahertz wave generation using a soliton microcomb. Opt Express 27:35257. https://doi.org/10.1364/OE.27.035257
162. Ye J, Hall JL, Diddams SA (2000) Precision phase control of an ultrawide-bandwidth femtosecond laser: a network of ultrastable frequency marks across the visible spectrum. Opt Lett 25:1675. https://doi.org/10.1364/OL.25.001675
163. Diddams SA, Udem T, Bergquist JC, et al (2001) An optical clock based on a single trapped 199Hg+ ion. Science 293:825–828. https://doi.org/10.1126/science.1061171
164. Diddams SA, Vahala K, Udem T (2020) Optical frequency combs: coherently uniting the electromagnetic spectrum. Science 369:eaay3676. https://doi.org/10.1126/science.aay3676

165. Spencer DT, Drake T, Briles TC, et al (2018) An optical-frequency synthesizer using integrated photonics. Nature 557:81–85. https://doi.org/10.1038/s41586-018-0065-7
166. Xu X, Tan M, Wu J, et al (2019) Microcomb-based photonic RF signal processing. IEEE Photonics Technol Lett 31:1854–1857. https://doi.org/10.1109/LPT.2019.2940497
167. Randel S, Kordts A, Freude W, et al (2018) Ultrafast optical ranging using microresonator soliton frequency combs. Science 359:887–891. https://doi.org/10.1126/science.aao3924
168. Suh M, Vahala K (2017) Soliton microcomb range measurement. 887:884–887. https://doi.org/10.1126/science.aao1968
169. Liu J, Tian H, Lucas E, et al (2020) Monolithic piezoelectric control of soliton microcombs. Nature 583:385–390. https://doi.org/10.1038/s41586-020-2465-8
170. Roztocki P, Morandotti R (2019) Astrocombs for extreme-precision spectroscopy. Nat Astron 3:135–136. https://doi.org/10.1038/s41550-019-0698-y
171. Liu L, Ye M, Yu Z (2020) Ultra-high peak rejection all-optical microwave filter based on the opto-mechanical rings. IEEE Photonics Technol Lett 1–1. https://doi.org/10.1109/LPT.2020.3013437
172. De Vos K, Bartolozzi I, Schacht E, et al (2007) Silicon-on-Insulator microring resonator for sensitive and label-free biosensing. Opt Express 15:7610. https://doi.org/10.1364/OE.15.007610
173. Tu X, Chen S-L, Song C, et al (2019) Ultrahigh Q polymer microring resonators for biosensing applications. IEEE Photonics J 11:1–10. https://doi.org/10.1109/JPHOT.2019.2899666
174. Kues M, Reimer C, Wetzel B, et al (2017) Passively mode-locked laser with an ultra-narrow spectral width. Nat Photonics 11:159–162. https://doi.org/10.1038/nphoton.2016.271
175. Tait AN, de Lima TF, Zhou E, et al (2017) Neuromorphic photonic networks using silicon photonic weight banks. Sci Rep 7:7430. https://doi.org/10.1038/s41598-017-07754-z
176. Feldmann J, Youngblood N, Wright CD, et al (2019) All-optical spiking neurosynaptic networks with self-learning capabilities. Nature 569:208–214. https://doi.org/10.1038/s41586-019-1157-8
177. Feldmann J, Youngblood N, Karpov M, et al (2020) Parallel convolution processing using an integrated photonic tensor core. 2002.00281v1
178. Miscuglio M, Sorger VJ (2020) Photonic tensor cores for machine learning. Appl Phys Rev 7:031404. https://doi.org/10.1063/5.0001942
179. Reimer C, Caspani L, Clerici M, et al (2014) Integrated frequency comb source of heralded single photons. Opt Express 22:6535. https://doi.org/10.1364/OE.22.006535
180. Roztocki P, Kues M, Reimer C, et al (2017) Practical system for the generation of pulsed quantum frequency combs. Opt Express 25:18940. https://doi.org/10.1364/OE.25.018940
181. Kues M, Reimer C, Roztocki P, et al (2017) On-chip generation of high-dimensional entangled quantum states and their coherent control. Nature 546:622–626. https://doi.org/10.1038/nature22986
182. Imany P, Jaramillo-Villegas JA, Odele OD, et al (2018) 50-GHz-spaced comb of high-dimensional frequency-bin entangled photons from an on-chip silicon nitride microresonator. Opt Express 26:1825. https://doi.org/10.1364/OE.26.001825
183. Reimer C, Sciara S, Roztocki P, et al (2019) High-dimensional one-way quantum processing implemented on d-level cluster states. Nat Phys 15:148–153. https://doi.org/10.1038/s41567-018-0347-x

184. Caspani L, Xiong C, Eggleton BJ, et al (2017) Integrated sources of photon quantum states based on nonlinear optics. Light Sci Appl 6:e17100–e17100. https://doi.org/10.1038/lsa.2017.100